Supporting Information

A novel multifunctional FePt/BP nanoplatform for synergistic Photothermal/Photodynamic/Chemodynamic cancer therapies and Photothermal enhanced Immunotherapy

Xiuxiu Yao[a,b], Baochan Yang[a,b], Shan Wang[a,b], Zhichao Dai[a], Dongsheng Zhang[a], , Iowan Zheng[a*], Qingyun Liu[b*]

[a.] Key Laboratory of Functional Nanomaterials and Technology in Universities of Shandong, College of Chemistry and Chemical Engineering, Linyi University, Linyi 276000, Shandong, P. R. China.

[b.] College of Chemical and Biological Engineering, Shandong University of Science and Technology, Qingdao 266590, Shandong, P. R. China.

*Corresponding authors: Xiuwen Zheng

Qingyun Liu

E-mail: zhengxiuwen@lyu.edu.cn

qyliu@sdust.edu.cn

Part of the experiment details

The rest of the material and the reagent

Octadecene (90%) and Oleylamine (>70%) were obtained from Aladdin. Meso-2, 3-Dimercaptosuccinic Acid (DMSA) was ordered from Sinopharm Chemical Reagent Co., Ltd. 1-Ethyl-3-carbodiimide hydrochloride (EDC, 97%) and Hydroxysuccinimide (NHS, 99%) were purchased from Xiya Reagent. Calcein (AM) and propidium iodide (PI) were from Yeasen Botech Co., ltd.

Characterization of Nanoparticles

The morphology of FePt, FePt-DMSA, BPNs, FePt /BPNs-PEI and FePt /BP-PEI-FA nanoparticles were characterized by JEOL JEM-2100 transmission electron microscopy (TEM) at 200 kV. The Zetasizer Nanoseries (Malvern Instruments, UK) was used to measure the zeta potential and hydrodynamic diameters of nanoparticles. High-angle annular dark-field (HAADF)-scanning transmission electron microscopy (STEM) equipped with elemental mapping was performed on a JEOL ARM-200F field emission transmission electron microscope. The UV-vis-NIR spectra of the materials were determined by Shimadzu 2700 Spectrophotometer, which scanned over the range of 200 - 850 nm. X-ray photoelectron spectroscopy (XPS) was performed using a Scientific Escalab 250 (Thermo, U.K.). FT-IR data was recorded on a Nicolet IR200 spectrophotometer. Fluorescence images were confirmed by Fluorescence Imager (Olympus). The temperature was recorded every 10 s by a thermal image device (FLIR Plus One 2, USA). ICP-MS (iCAP Qc, Thermo Fisher) method was used to determine the Fe content. MR imaging were obtained by a MRI scanner (GE Sigma HDx 3.0 T

MRI, USA).

Determine the weight ratio of PEI and FA in FePt/BP-PEI-FA

UV-vis absorption spectra of pure FA at different concentrations (8.90, 11.0, 13.3, 18.92, 25.0, 33μg mL^{-1}) and PEI at different concentrations (27.8, 33.3, 38.9, 100, 133μg mL^{-1}) (Fig S4a and S4c) were measured. Then the C_{FA}-Absorbance standard curves based on absorbance intensity at 280 nm of FA (Fig S4b) and the C_{PEI}-Absorbance standard curves based on absorbance intensity at 204 nm of PEI (Fig S4d) were obtained. Finally, the quality of FA were determined according to the difference in UV-vis absorption value of FePt/BP-PEI before and after supported by FA, and the quality of PEI were measured according to the difference between the absorption value of BP-PEI with BP(Fig. 2B). After calculation, the quality of PEI and FA are 1644 and 437.4μg respectively.

Calculation of the photothermal conversion efficiency of FePt/BP-PEI-FA

The photothermal conversion efficiency (η) can be calculated from the data in Figure S5 a according to previously published literature using the following formula.

$$\eta = \frac{hS\left(T_{max} - T_{surr}\right) - Q_{dis}}{I\left(1 - 10^{-A_{808}}\right)}$$

where h is the heat transfer coefficient, S is the surface area of the container, T_{max} is the equilibrium temperature, T_{surr} is the environment temperature, Q_{dis} is the heat dissipated from light absorbed by the container itself, I is the laser power used in the experiment, A_{808} is the absorbance of FePt/BP PEI-FA solution at 808 nm.

T_{max} = 54.3℃, T_{surr} = 22.6 ℃, I = 1.75 W cm^{-2}, A_{808} = 0.76, Q_{dis} = (5.4◊10^{-4}) I=0.95 mW.

hS is calculated according to the following equation

$$hS = \frac{m_w c_w}{\tau_s}$$

m_w represents the mass of water (0.5 g), c_w is the heat capacity of water (4.2 J/g), τ_s is the time constant of the sample system.

To determine τ_s, a dimensionless driving force temperature θ is introduced, which is defined by

$$\theta = \frac{T - T_{surr}}{T_{max} - T_{surr}}$$

$$t = \tau_s\,(-ln\theta)$$

where T is the real-time temperature of the nanomaterials when the laser was turned off, t represents time. As can be seen from Figure S5 b, τ_s is determined to be 146.31s. Thus, the photothermal conversion efficiency is obtained:

$$\eta = \frac{0.5\frac{4.2}{146.31}(54.3 - 22.6) - 0.0009}{1.75\,(1 - 10^{-0.755})} = 31.40\%$$

Cell Culture

The $4T_1$ (mouse mammary carcinoma cell lines), MCF-7 (human breast carcinoma cell lines), L02 (human hepatocyte cell lines) were originally from the Cell Bank of Chinese Academy of Science. All the cells were cultured in complete medium that containing Dulbecco's modified Eagle's medium (DMEM) medium, 10 % fetal bovine serum and 1 % penicillin-streptomycin at 37 °C incubator containing 5% CO_2.

In vitro Cell Cytotoxicity Assay

The cell cytotoxicity of FePt/BP-PEI-FA was measured on L02, $4T_1$, Hela and MCF-7

cells, respectively. Specifically, the cells were co-cultured with various concentration of FePt/BP-PEI-FA ([Fe] = 0, 7.17, 14.34, 21.51, 28.68, 35.85 μg mL^{-1}). After 8 h, the noninternalized nanomaterials was discarded and CCK-8 reagents was used to monitor the survival rates. For in vitro synergistic PTT/PDT/CDT treatments, $4T_1$ cells were treated with free BPNs, FePt NPs, FePt/BP-PEI-FA nanocomposites at a half-maximum inhibitory concentration (IC_{50}) of Fe of 25 μg mL^{-1}, the cell death rates were evaluated after different treatments: FePt NPs irradiated with 808 nm and 660 nm laser; BPNs with the same laser treatments; FePt/BP-PEI-FA NCs with 808 nm laser alone; FePt/BP-PEI-FA NCs with 660 nm laser alone; FePt/BP-PEI-FA NCs with 808 nm and 660 nm laser. Both the 808 nm laser with pump power of 1.75 W cm^{-2} and 660 nm laser with pump power of 0.3 W cm^{-2} were irradiated for 5 min. The cells were further incubated for another 3 h and then survival rates were investigated. For confocal imaging, $4T_1$ cancer cells were stained by calcein AM and PI and then imaged using a Leica SP5 laser scanning confocal microscope. Moreover, after incubating $4T_1$ cells with FePt/BP-PEI-FA for 8 h, GSH (5 mM), Cys (5 mM), Glu (5 mM), VC (100 μM), and VE (100 μM) was added, respectively, and incubated for another 30 min, the CCK-8 assay was conducted.

ROS Detection

In order to testify the intracellular production of ROS, $4T_1$ cells were added in 24-well assay plates and cultured in prepared complete medium. BPNs, FePt NPs and FePt/BP-PEI-FA NCs (IC_{50}, [Fe] = 25 μg mL^{-1}) were added and incubated for 8 h. Suspension was discarded, and 1 mL of basic DMEM medium with 10 μM DCFH-DA was added

and incubated for another 20 min. After washing three times with PBS, The materials were treated with or without 660 nm laser (0.3 W cm^{-2}, 5 min). Finally, the fluorescence signals of cells (λex / λem = 488/520 nm) were recorded at the same real exposure time. The fluorescence image was acquired by an Olympus digital camera. For the generation of $^1O_2$, 10 μL (50 μM) H_20_2 and SOSG (10 μL, 0.5×10^{-3} m) were added into dispersion that containing FePt/BP-PEI-FA NCs ([Fe] = 25 μg mL^{-1}). The samples were continuously treated with or without 660 nm laser irradiation (0.3 W cm^{-1}) for 30 min. The fluorescence intensity of SOSG was acquired by a spectrofluorophotometer with excitation at 494 nm every 5 min.

Intratumoral Injection of Different Materials for Screening Test

Female balb/c mice were purchased from Jinan Peng Yue Biological Technology Co Ltd. and all animal experiments were proceeded under the protocols approved by Qilu Hospital Laboratory Animal Center. Screening test was carried out to find out the nanomaterials with the best anti-tumor effects. $4T_1$ cells (1×10^6) injected subcutaneously into the right hind leg of mice to establish tumor models. Mice with an initial tumor volume of 150 mm^3 were divided into nine groups (n=3) and intratumoral injected according to the following treatments: PBS (Group 1, 100 μL); BPNs (Group 2, 100 μg mL^{-1}, 100 μL), BPNs + 808 nm + 660 nm laser irradiation (Group 3, 100 μg mL^{-1}, 100 μL); FePt NPs (Group 4, [Fe] = 250 μg mL^{-1}, 100 μL), FePt NPs + 808 nm + 660 nm laser irradiation (Group 5, [Fe] = 250 μg mL^{-1}, 100 μL); FePt/BP-PEI-FA NCs (Group 6, [Fe] = 250 μg mL^{-1}, 100 μL); FePt/BP-PEI-FA NCs + 660 nm laser irradiation (Group 7, [Fe] = 250 μg mL^{-1}, 100 μL); FePt/BP-PEI-FA NCs + 808 nm

laser irradiation (Group 8, [Fe] = 250 μg mL^{-1}, 100 μL) and FePt/BP-PEI-FA NCs + 808 nm + 660 nm laser irradiation (Group 9, [Fe] = 250 μg mL^{-1}, 100 μL). Both the 808 nm laser (1.75 W cm^{-2}) and 660 nm laser (0.3 W cm^{-2})were irradiated for 5 min. Mice were injected intratumoral every three days for five times. During this period, the mouse weight and tumor volume changes were monitored every two days.

In Vivo Pharmacokinetics and Biodistribution

To study the pharmacokinetics of particles, tumor-bearing mice (n=3) received an intravenous (i.v.) injection of FePt/BP-PEI-FA ([Fe] = 250 μg mL^{-1}, 100 μL). The Fe concentration in blood at various time points was quantified with ICP-MS. To study the biodistribution of nanomaterials in various organs, mice were euthanized at 24h postinjection, major organs were collected and then Fe content was quantified with ICP-MS.

In Vitro and In Vivo T_2-Weighted MR Imaging

All in vitro and in vivo T_2-weighted MR studies were performed by a 3.0 T clinical MRI scanner. In brief, for in vitro MR imaging, FePt/BP-PEI-FA NCs with various Fe concentrations were placed in 2 mL centrifuge tubes. The r_2 relaxivity values were acquired by the curve fitting of $1/T_2$ relaxation time (s^{-1}) versus the Fe concentration. In vivo, the 100 μL of FePt/BP-PEI-FA NCs ([Fe] = 250 μg mL^{-1}) of concentration were injected intravenously into tumor-bearing mice and MR imaging were recorded at 0, 1, 2, 4 and 7 h respectively.

Histological Assessments

After various treatment by intravenous injection, the major organs (heart, liver, spleen, lung and kidney) as well as tumors in all groups were acquired and stained with hematoxylin and eosin (H&E), finally observed under a digital microscope (Olympus BX51).

DCs Maturation detected by flow cytometry

Mice were treated with following treatments: PBS (Group 1, 150 uL); FePt/BP-PEI-FA NCs (Group 2, [Fe] = 250 μg mL^{-1}, 100 μL); FePt/BP-PEI-FA NCs (Group 3, [Fe] = 250 μg mL^{-1}, 100 μL, 808 nm pump power of 1.75 W cm^{-2}). After three times intravenous injection, the lymph nodes were obtained and single dispersed cells were isolated by standard method, and the cells were dyed with anti-CD11c APC, anti-CD86 PE and anti-CD80 FITC. Finally the maturation of DCs were detected by flow cytometry.

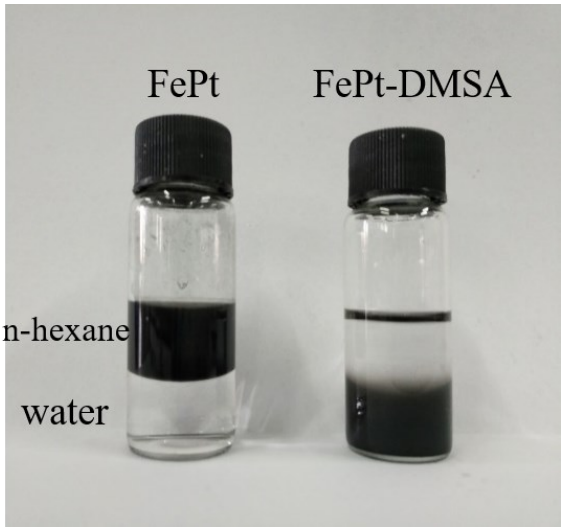

Fig S1. The image of FePt NPs before and after transferred from lipophilic to hydrophilic by DMSA.

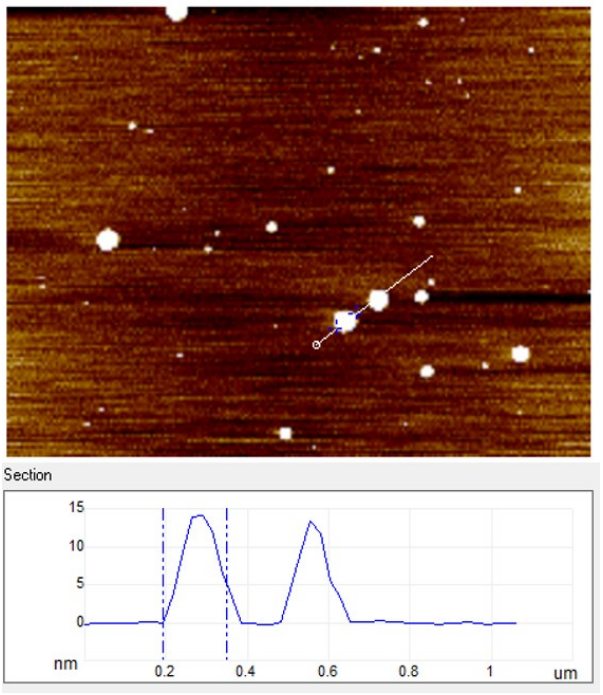

Fig S2. The Atomic force microscopy (AFM) micrograph of BP nanosheets.

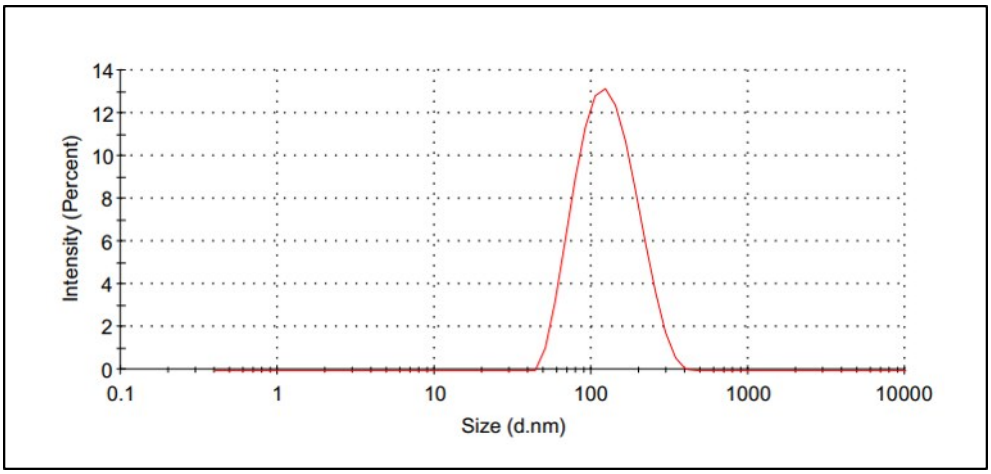

Fig S3. The dynamic light scattering (DLS) size of FePt/BP-PEI-FA nanocomposite

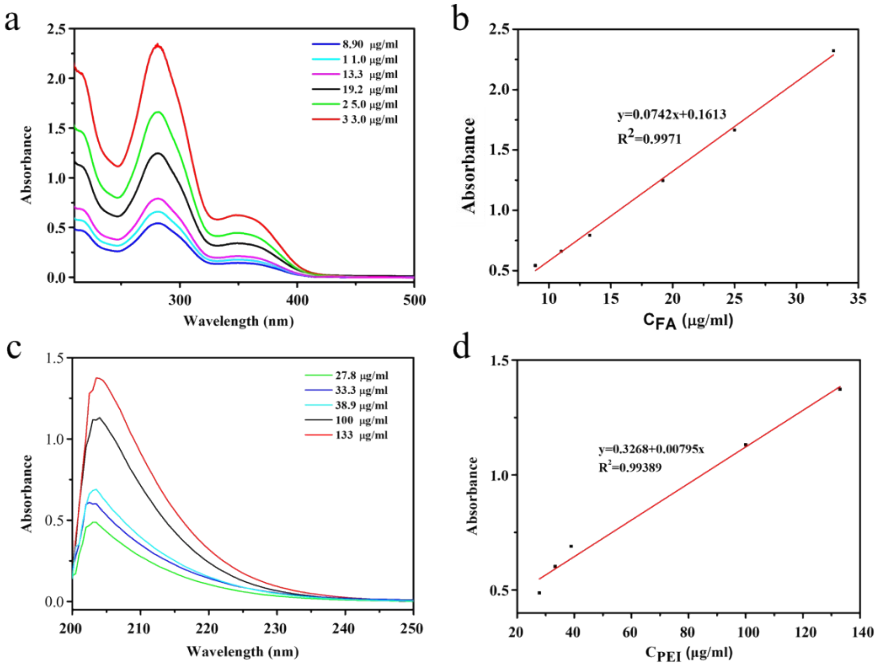

Fig S4. The exploration of quality of FA and PEI in FePt/BP-PEI-FA. (a) UV−vis absorption spectra of FA at different concentration. (b) The standard coordinate line of intensity at 280 nm of FA of (a). (c) UV−vis absorption spectra of PEI at different concentration. (d) The standard coordinate line of intensity at 204 nm of PEI of (c).

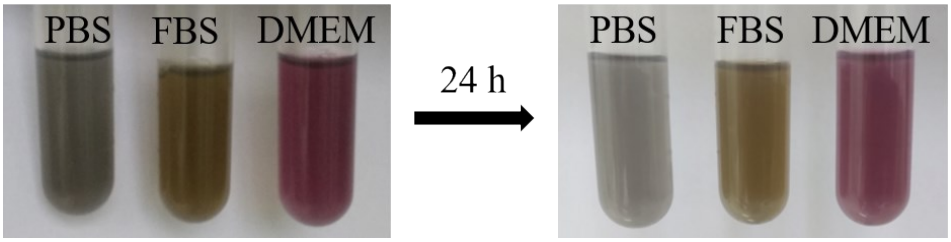

Fig S5. Stabilities of the nanomaterials dissolved in PBS, FBS and DMEM for 24 h, respectively.

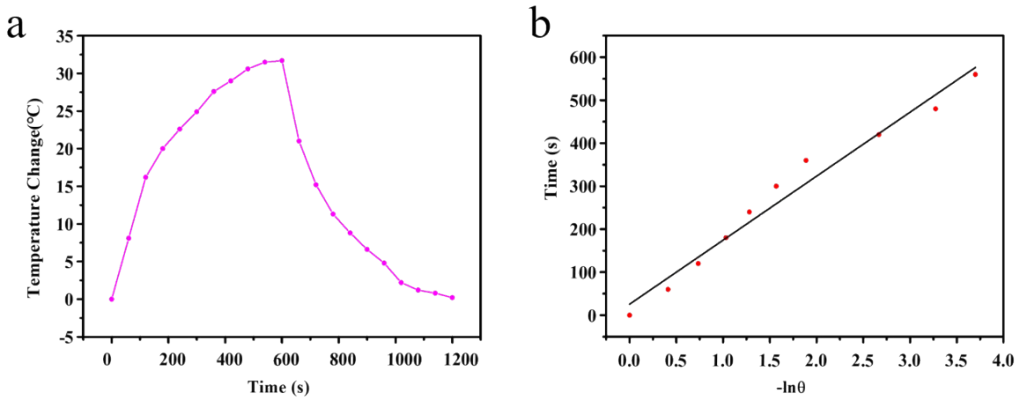

Fig S6. (a) Temperature of FePt/BP-PEI-FA NCs under one laser on-off cycle. (b) Time constant for heat transfer from the system is measured by using a linear time data from the cooling period versus negative natural logarithm of driving force temperature.

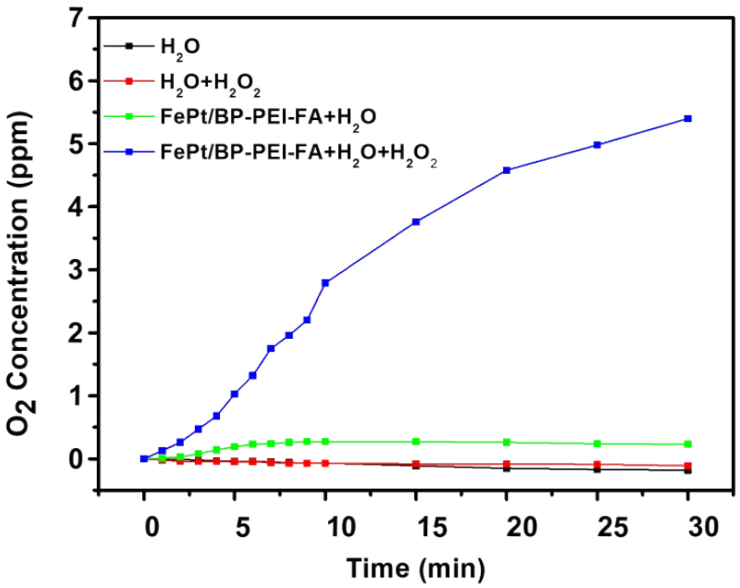

Fig S7. The generation of O_2 under various treatments: H_2O, H_2O + H_2O_2, FePt/BP-PEI-FA NCs + H_2O, FePt/BP-PEI-FA NCs + H_2O+ H_2O_2.

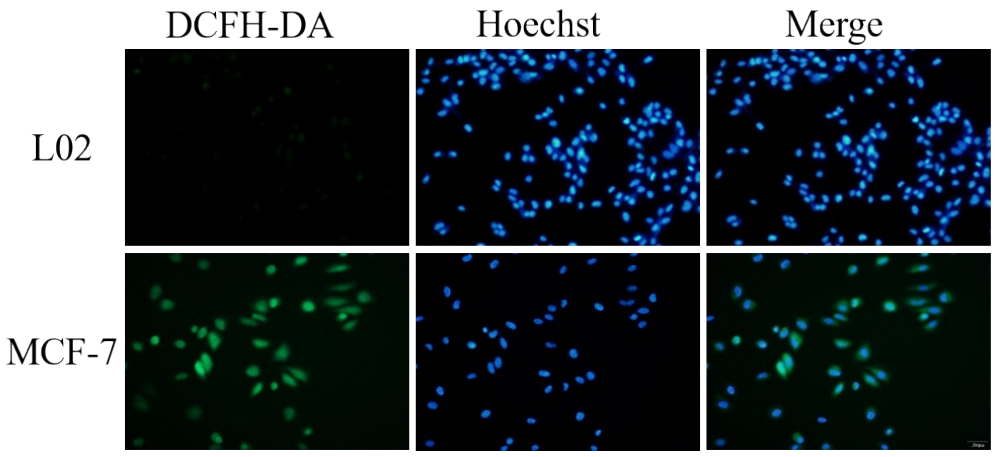

Fig S8. The fluorescence image of FePt/BP-PEI-FA NCs co-cultured with L02 and MCF-7 cells for ROS detection.

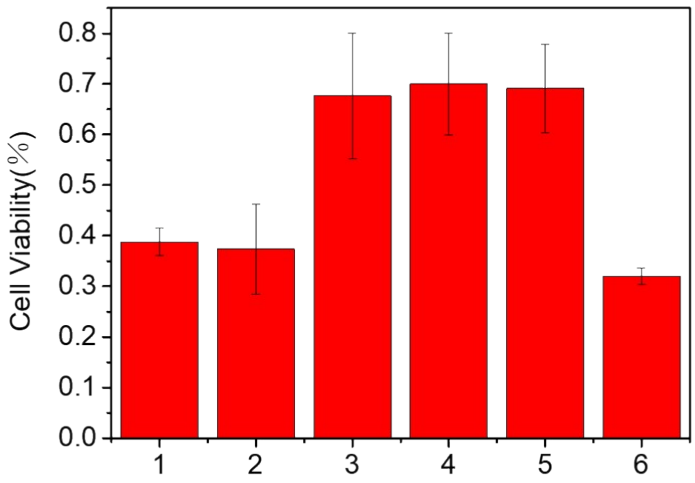

Fig S9. Survival rates of $4T_1$ cells incubated with FePt/BP-PEI-FA NCs, FePt/BP-PEI-FA NCs + VC, FePt/BP-PEI-FA NCs + VE, FePt/BP-PEI-FA NCs + GSH, FePt/BP-PEI-FA NCs + Cys, FePt/BP-PEI-FA NCs + Glu, respectively.

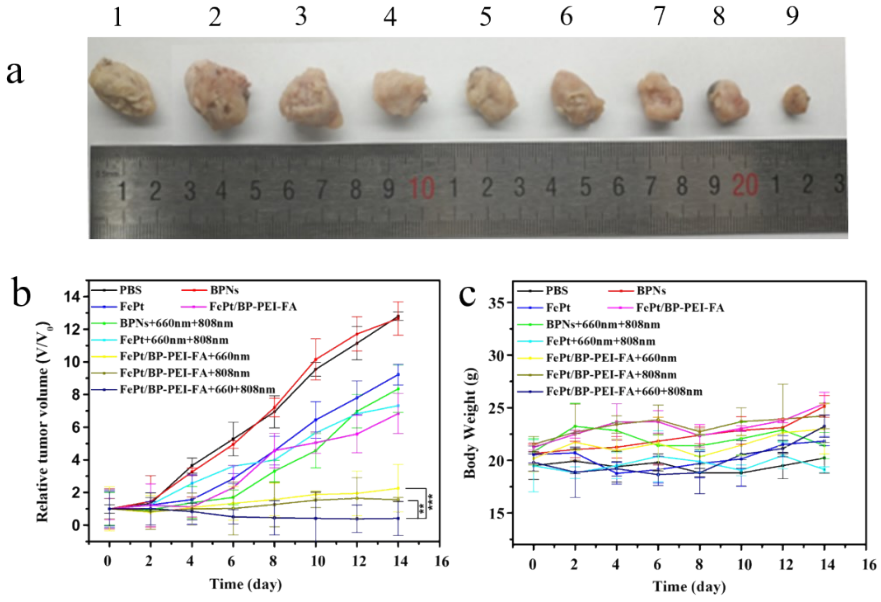

Fig S10. (a) The picture of the tumors in all groups after different treatments via intratumor injection (The data points represent mean ± s.d; **p < 0.01, ***p < 0.001, n=3). (b) The volume of tumors in tumor-bearing mice during different treatments. (c) The body weight of mice during different treatments.

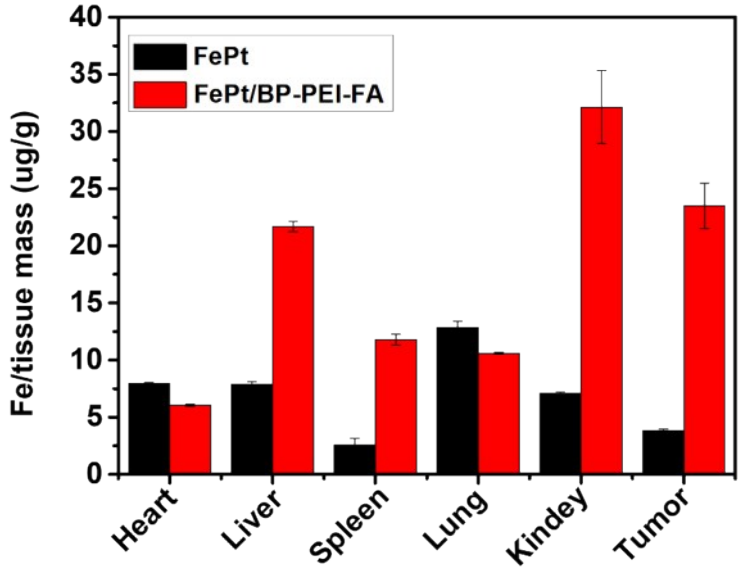

Fig S11. Biodistribution of the nanoparticles 24 h after intratumor injection into tumor-bearing mice. The Fe content were measured by using ICP-MS.

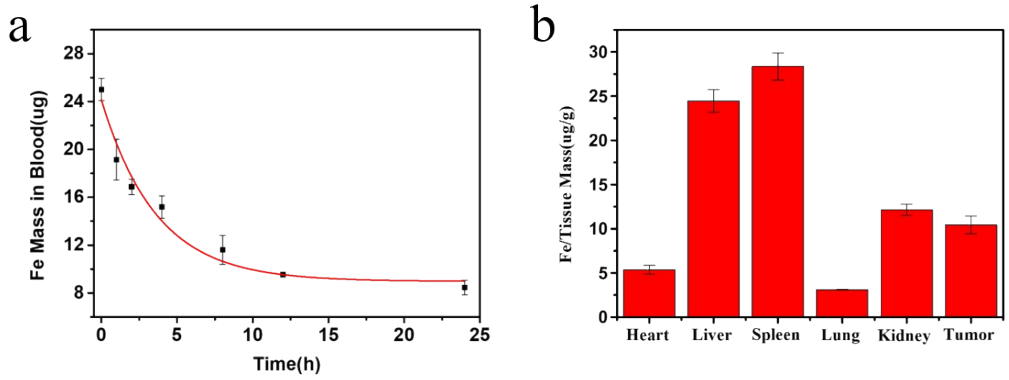

Fig S12. (a) Pharmacokinetics curves over a span of 24 h after intravenous injection of FePt/BP-PEI-FA NCs into tumor-bearing mice. (b) Biodistribution of the nanoparticles 24 h after intratumor injection into tumor-bearing mice. The Fe content were measured by using ICP-MS.

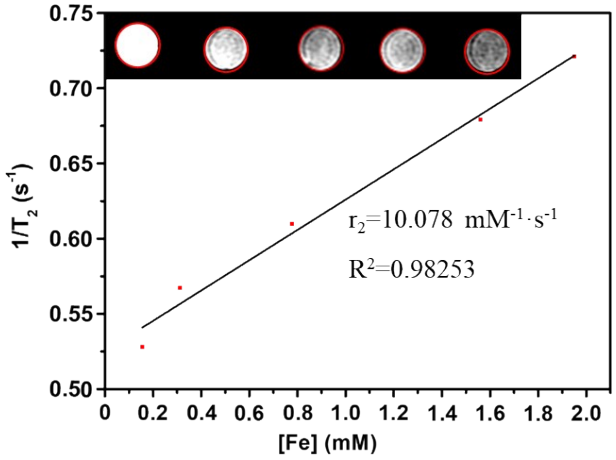

Fig S13 In vitro T_2 relaxation rate of FePt/BP-PEI-FA NCs under various Fe concentration. Insert: MR images of different concentration of FePt/BP-PEI-FA NCs.

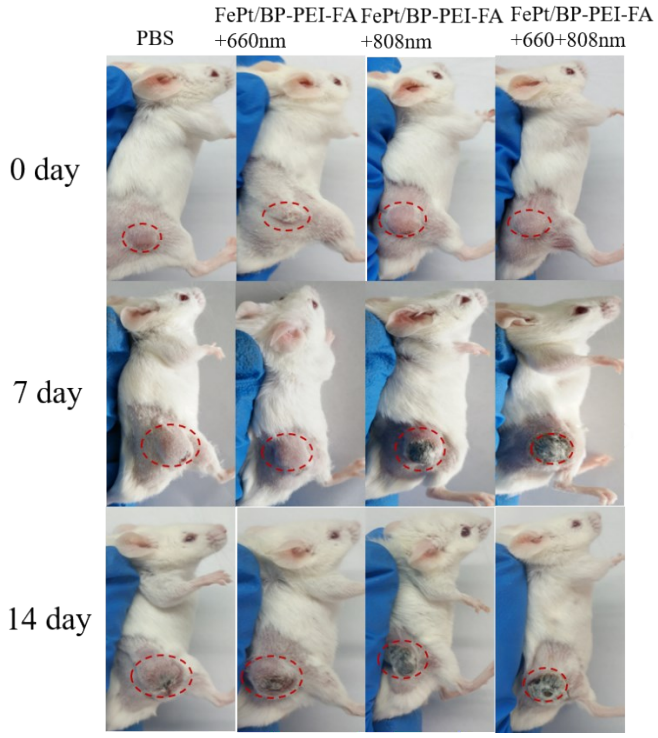

Fig S14. The pictures of tumor sites on day 0, 7 and day 14 of mice under different treatments.

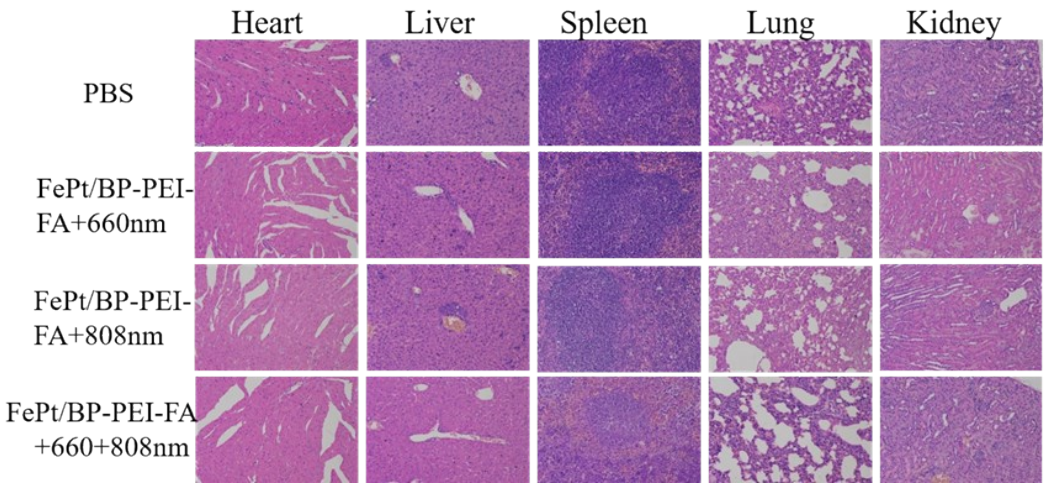

Fig S15. H&E assay images of major organs after different treatments.

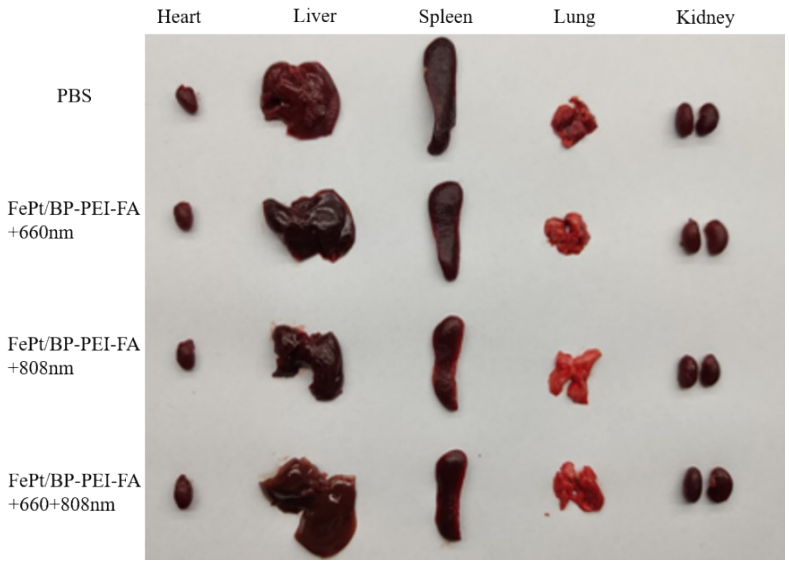

Fig S16. The picture of the major organs of the mice treated with different treatments by using intravenous injection.

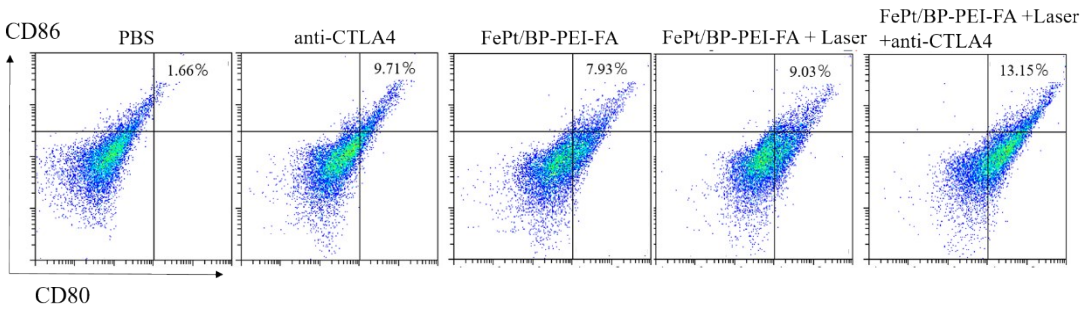

Fig S17. The percent of DC maturation after different treatments. After staining with CD11c, CD80, and CD86, cells in distant tumors were measured by flow cytometry.

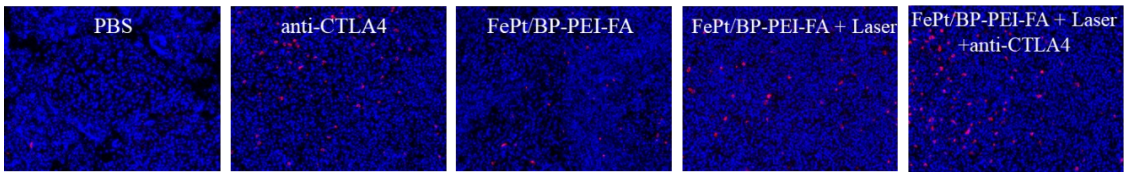

Fig S18. T cell immunofluorescence assay. Bilateral tumor models were established and treated with PBS, anti-CTLA4, FePt/BP-PEI-FA, FePt/BP-PEI-FA + Laser (808 nm, 1.75 W·cm^{-2}, 5 min) and FePt/BP-PEI-FA + Laser + anti-CTLA4, respectively. 10 days after the first treatment, distant tumors were collected, sectioned and subjected to immunofluorescence staining. Representative CLSM images of tumors after immunofluorescence staining. Red fluorescence indicates $CD8^+$ T cells. Scale bar: 100 μm.

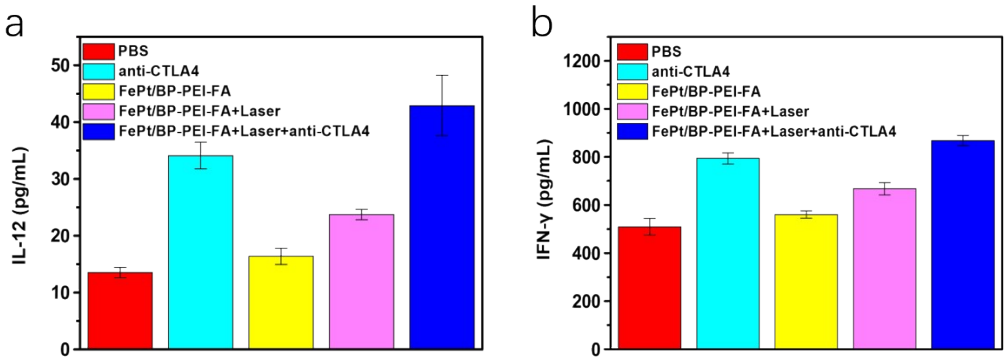

Fig S19. Secretion of IL-12 and IFN-γ in tumor cell suspensions after different treatments**.**

Table

Table S1. Mass ratio and Atomic ratio of FePt/BP-PEI-FA

	Mass ratio	Atomic ratio
Fe	0.38	0.09
Pt	1.76	0.13
P	0.30	0.14